NACA RM L51K15a

NACA

RESEARCH MEMORANDUM

AERODYNAMIC CHARACTERISTICS AT SUPERSONIC SPEEDS OF A SERIES OF WING-BODY COMBINATIONS HAVING CAMBERED WINGS WITH AN ASPECT RATIO OF 3.5 AND A TAPER RATIO OF 0.2

EFFECTS OF SWEEP ANGLE AND THICKNESS RATIO ON THE STATIC LATERAL STABILITY CHARACTERISTICS AT M = 1.60

By M. Leroy Spearman and John H. Hilton, Jr.

Langley Aeronautical Laboratory
Langley Field, Va.

NATIONAL ADVISORY COMMITTEE
FOR AERONAUTICS
WASHINGTON

January 21, 1952
Declassified May 16, 1958

NATIONAL ADVISORY COMMITTEE FOR AERONAUTICS

RESEARCH MEMORANDUM

AERODYNAMIC CHARACTERISTICS AT SUPERSONIC SPEEDS OF A SERIES OF WING-BODY COMBINATIONS HAVING CAMBERED WINGS WITH AN ASPECT RATIO OF 3.5 AND A TAPER RATIO OF 0.2

EFFECTS OF SWEEP ANGLE AND THICKNESS RATIO ON THE STATIC LATERAL STABILITY CHARACTERISTICS AT $M = 1.60$

By M. Leroy Spearman and John H. Hilton, Jr.

SUMMARY

An investigation has been conducted in the Langley 4- by 4-foot supersonic pressure tunnel at a Mach number of 1.60 and a Reynolds number of 2.7×10^6, based on the wing mean aerodynamic chord, to determine the effects of sweep angle and thickness ratio on the static lateral stability characteristics of a series of wing-body combinations having cambered wings of aspect ratio 3.5 and taper ratio 0.2. The wings, tested on a body of revolution, had quarter-chord sweep angles of 10.8°, 35°, and 47° with a thickness ratio of 4 percent, and thickness ratios of 4, 6, and 9 percent with a sweep angle of 47°. The effects of a nacelle installation on the 6-percent-thick 47° swept wing were also investigated. The results of these tests show the effects of sweep, thickness, and the nacelle installation on the static lateral stability characteristics.

INTRODUCTION

A research program has been in progress at the Langley Aeronautical Laboratory to determine at subsonic, transonic, and supersonic speeds, the effects of thickness and sweep on the aerodynamic characteristics of a series of wing-body combinations with cambered wings having a taper ratio of 0.2 and an aspect ratio of 3.5. The effects of thickness on the longitudinal characteristics of a 47° sweepback wing-body combination at subsonic and transonic speeds are presented in reference 1. The effects of sweep and thickness on the longitudinal characteristics for the series of wings at a Mach number of 1.60 are presented in reference 2. The results of tests of several nacelle installations on a 47° sweptback wing are presented in reference 3.

As a part of this research program, the present paper reports the results of an investigation made to determine some effects of sweep and thickness on the static lateral stability characteristics of this series of wing-body combinations at a Mach number of 1.60 and a Reynolds number of 2.7×10^6 based on the wing mean aerodynamic chord. The wings had quarter-chord sweep angles of 10.8°, 35°, and 47° with a thickness ratio of 4 percent, and thickness ratios of 4, 6, and 9 percent with a sweep angle of 47°. In addition, the effects of a nacelle installation on the 6-percent-thick 47° sweptback wing were investigated. The results are presented without analysis to expedite issuance.

COEFFICIENTS AND SYMBOLS

The results of the tests are presented as standard NACA coefficients of forces and moments. The data are referred to the stability-axes system (fig. 1) with the reference center of gravity at 25 percent of the wing mean aerodynamic chord.

The coefficients and symbols are defined as follows:

C_Y lateral-force coefficient (Y/qS)

C_n yawing-moment coefficient (N/qSb)

C_l rolling-moment coefficient (L/qSb)

C_L lift coefficient $(-Z/qS)$

C_X longitudinal-force coefficient (X/qS)

C_m pitching-moment coefficient $(M'/qS\bar{c})$

X force along X-axis

Y force along Y-axis

Z force along Z-axis

L moment about X-axis

M'	moment about Y-axis
N	moment about Z-axis
q	free-stream dynamic pressure
S	total wing area
b	wing span
$\bar{c}$	wing mean aerodynamic chord
M	Mach number
t/c	thickness ratio (Wing thickness/Wing chord)
α	angle of attack of body center line, degrees
ψ	angle of yaw, degrees
Λ	angle of sweep of wing quarter-chord line, degrees
C_{Y_ψ}	lateral-force parameter, rate of change of lateral-force coefficient with angle of yaw $(\partial C_Y/\partial\psi)$
C_{n_ψ}	directional-stability parameter, rate of change of yawing-moment coefficient with angle of yaw $(\partial C_n/\partial\psi)$
C_{l_ψ}	effective-dihedral parameter, rate of change of rolling-moment coefficient with angle of yaw $(\partial C_l/\partial\psi)$

APPARATUS AND MODELS

Tunnel

The tests were conducted in the Langley 4- by 4-foot supersonic pressure tunnel. This tunnel, described in reference 4, was originally powered by a 6000-horsepower drive motor. Recent modifications to the tunnel have increased the horsepower rating to 45,000. The additional power has resulted in an increase in the maximum stagnation pressure from 0.3 atmosphere to about 2 atmospheres. The design Mach number range of 1.2 to 2.2 remains unchanged. At a Mach number of 1.60, the test section has a width of 4.5 feet, a height of 4.4 feet, and a region of uniform flow which is 7 feet long at the flexible walls. An external air-drying system supplies air of a sufficiently low dew point to prevent moisture condensation in the test section.

Models

The models used in these tests were composed of an ogive-cylinder body and various midwing configurations with a ratio of body diameter to wing span of about 0.094. The models were designed to accommodate solid steel wings with integral cylindrical sections simulating corresponding sections of the body. This design permitted interchange of wings with minimum delay. The wings were positioned so that the quarter-chord point of the mean aerodynamic chord was always at the same body station. The wing airfoil sections had an NACA 65A-series thickness distribution with mean line ordinates one-third of NACA 230 plus (a = 1) for $C_L = 0.1$. The airfoil coordinates are given in table I. Details of the models are shown in figure 2.

The models were sting-supported and had a six-component internal strain-gage balance in the body. The model and sting are shown in figure 3. The models, balance, and indicating systems were furnished by a U. S. Air Force contractor.

TESTS

Test Conditions

The conditions for the tests were:

Mach number	1.60
Reynolds number, based on wing mean aerodynamic chord	2.7×10^6
Stagnation dew point, degrees Fahrenheit	<-25
Stagnation pressure, atmosphere	1
Stagnation temperature, degrees Fahrenheit	110

A limited calibration prior to those tests has shown that the flow in the test section is reasonably uniform. The magnitudes of the variations in the flow parameters are summarized in the following table:

Flow parameter	Magnitude (deg)
Mach number	±0.01
Flow angle in horizontal plane	±.1
Flow angle in vertical plane	±.1

Test Procedure

Tests were made through an angle-of-yaw range from -2° to 10° at an angle of attack of 5° and through an angle-of-attack range from -2° to 12° at angles of yaw of 0° and 5°.

Corrections and Accuracy

The angles of attack and yaw were corrected for the deflection of the balance under load. The estimated accuracy of both the angle of attack and angle of yaw was $\pm 0.1^\circ$. No corrections were applied to the data to account for the flow variations in the test section.

The estimated errors in the force data were as follows:

C_L	±0.005
C_D	±.001
C_m	±.001
C_Y	±.003
C_n	±.0003
C_l	±.0002

The base pressure was measured and the drag data were corrected to correspond to a base pressure equal to the free-stream static pressure.

RESULTS

The results are presented in this paper without analysis in order to expedite publication. The aerodynamic characteristics in yaw for various configurations at $\alpha = 5^\circ$ are presented in figure 4. The effects of yaw on the lateral characteristics in pitch for various configurations are shown in figure 5. The static lateral stability characteristics of the various configurations at $\alpha = 5^\circ$ are summarized in table II and are presented as functions of sweep angle and thickness ratio in figure 6.

Although these data are presented without analysis, some general remarks can be made. Both C_{Y_ψ} and C_{n_ψ} are essentially invariant with lift coefficient. The effect of increasing the sweep angle or thickness ratio is to increase the positive value of C_{Y_ψ} and decrease the positive value of C_{n_ψ}. The effective dihedral C_{l_ψ}, although quite small, appears to change from negative to positive as the lift coefficient increases. The effect of the nacelle installation is to increase the positive value of C_{Y_ψ} and C_{n_ψ} and to produce a negative value of C_{l_ψ}.

Langley Aeronautical Laboratory
National Advisory Committee for Aeronautics
Langley Field, Va.

REFERENCES

1. Bielat, Ralph P., Harrison, Daniel E., and Coppolino, Domenic A.: An Investigation at Transonic Speeds of the Effects of Thickness Ratio and of Thickened Root Sections on the Aerodynamic Characteristics of Wings with 47° Sweepback, Aspect Ratio 3.5, and Taper Ratio 0.2 in the Slotted Test Section of the Langley 8-Foot High-Speed Tunnel. NACA RM L51I04a, 1951.

2. Robinson, Ross B., and Driver, Cornelius: Aerodynamic Characteristics at Supersonic Speeds of a Series of Wing-Body Combinations Having Cambered Wings with an Aspect Ratio of 3.5 and a Taper Ratio of 0.2. Effects of Sweep Angle and Thickness Ratio on the Aerodynamic Characteristics in Pitch at $M = 1.60$. NACA RM L51K16a, 1951.

3. Hasel, Lowell E., and Sevier, John R., Jr.: Aerodynamic Characteristics at Supersonic Speeds of a Series of Wing-Body Combinations Having Cambered Wings with an Aspect Ratio of 3.5 and a Taper Ratio of 0.2. Effect at $M = 1.60$ of Nacelle Shape and Position on the Aerodynamic Characteristics in Pitch of Two Wing-Body Combinations with 47° Sweptback Wings. NACA RM L51K14a, 1951.

4. Cooper, Morton, Smith, Norman F., and Kainer, Julian H.: A Pressure-Distribution Investigation of a Supersonic Aircraft Fuselage and Calibration of the Mach Number 1.59 Nozzle of the Langley 4- by 4-Foot Supersonic Tunnel. NACA RM L9E27a, 1949.

TABLE I

AIRFOIL COORDINATES FOR THE VARIOUS WINGS

[Thickness distribution: NACA 65A-series. Mean-line ordinates: one-third of NACA 230 + (a = 1) for $C_L = 0.1$]

(a) $\frac{t}{c} = 0.04$

x/c	y/c Upper surface	y/c Lower surface
0	0	0
.5	.411	.245
.75	.499	.271
1.25	.665	.289
2.5	.962	.324
5.0	1.435	.367
7.5	1.776	.429
10	2.039	.472
15	2.423	.577
20	2.642	.682
25	2.800	.787
30	2.887	.892
35	2.983	.997
40	2.992	1.006
45	2.940	1.041
50	2.852	1.006
55	2.712	.945
60	2.511	.857
65	2.265	.761
70	1.986	.674
75	1.680	.577
80	1.356	.481
85	1.041	.385
90	.726	.289
95	.402	.201
100	.105	.105
Tangent point	80.00	60.00
L.E. radius = 0.0016c		

(b) $\frac{t}{c} = 0.06$

x/c	y/c Upper surface	y/c Lower surface
0	0.061	0
.5	.577	.376
.75	.717	.446
1.25	.919	.534
2.5	1.304	.621
5.0	1.872	.761
7.5	2.318	.857
10	2.668	.980
15	3.150	1.269
20	3.482	1.496
25	3.701	1.697
30	3.858	1.846
35	3.946	1.960
40	3.981	2.021
45	3.937	2.030
50	3.823	1.977
55	3.613	1.872
60	3.342	1.697
65	3.018	1.487
70	2.651	1.277
75	2.231	1.059
80	1.785	.849
85	1.339	.639
90	.892	.420
95	.446	.210
100	0	0
L.E. radius = 0.0024c		

(c) $\frac{t}{c} = 0.09$

x/c	y/c Upper surface	y/c Lower surface
0	0.156	0
.5	.846	.574
.75	1.021	.680
1.25	1.283	.846
2.5	1.789	1.069
5.0	2.537	1.400
7.5	3.111	1.662
10	3.577	1.896
15	4.244	2.352
20	4.705	2.751
25	5.045	3.052
30	5.288	3.276
35	5.415	3.441
40	5.473	3.529
45	5.424	3.519
50	5.249	3.422
55	4.967	3.208
60	4.579	2.916
65	4.102	2.566
70	3.568	2.197
75	2.975	1.837
80	2.382	1.468
85	1.789	1.098
90	1.186	.739
95	.593	.369
100	0	0
L.E. radius = 0.0056c		

(d) Thickened root

x/c	Root station y/c Upper surface	Root station y/c Lower surface
0	0.301	0
.5	1.120	.754
.75	1.335	.904
1.25	1.658	1.141
2.5	2.261	1.507
5.0	3.208	2.024
7.5	3.919	2.433
10	4.500	2.799
15	5.362	3.445
20	5.965	3.984
25	6.395	4.414
30	6.718	4.716
35	6.912	4.910
40	6.977	5.017
45	6.912	4.996
50	6.675	4.823
55	6.288	4.522
60	5.771	4.113
65	5.168	3.618
70	4.457	3.101
75	3.725	2.584
80	2.929	2.067
85	2.239	1.550
90	1.486	1.034
95	.732	.517
100	0	0
L.E. radius = 0.0099c		

TABLE II

SUMMARY OF STATIC LATERAL STABILITY DERIVATIVES

Λ (deg)	t/c	Nacelle	$C_{Y_{\psi}}$	$C_{n_{\psi}}$	$C_{l_{\psi}}$
10.8	0.04	Off	0.0012	0.00057	-0.00010
35	.04		.0018	.00046	0
47	.04		.0020	.00040	.00003
47	.06		.0022	.00030	-.00003
47	.09		.0026	.00017	-.00011
47	.06	On	.0076	.00122	-.00020
Body alone			.0015	.00055	.00004

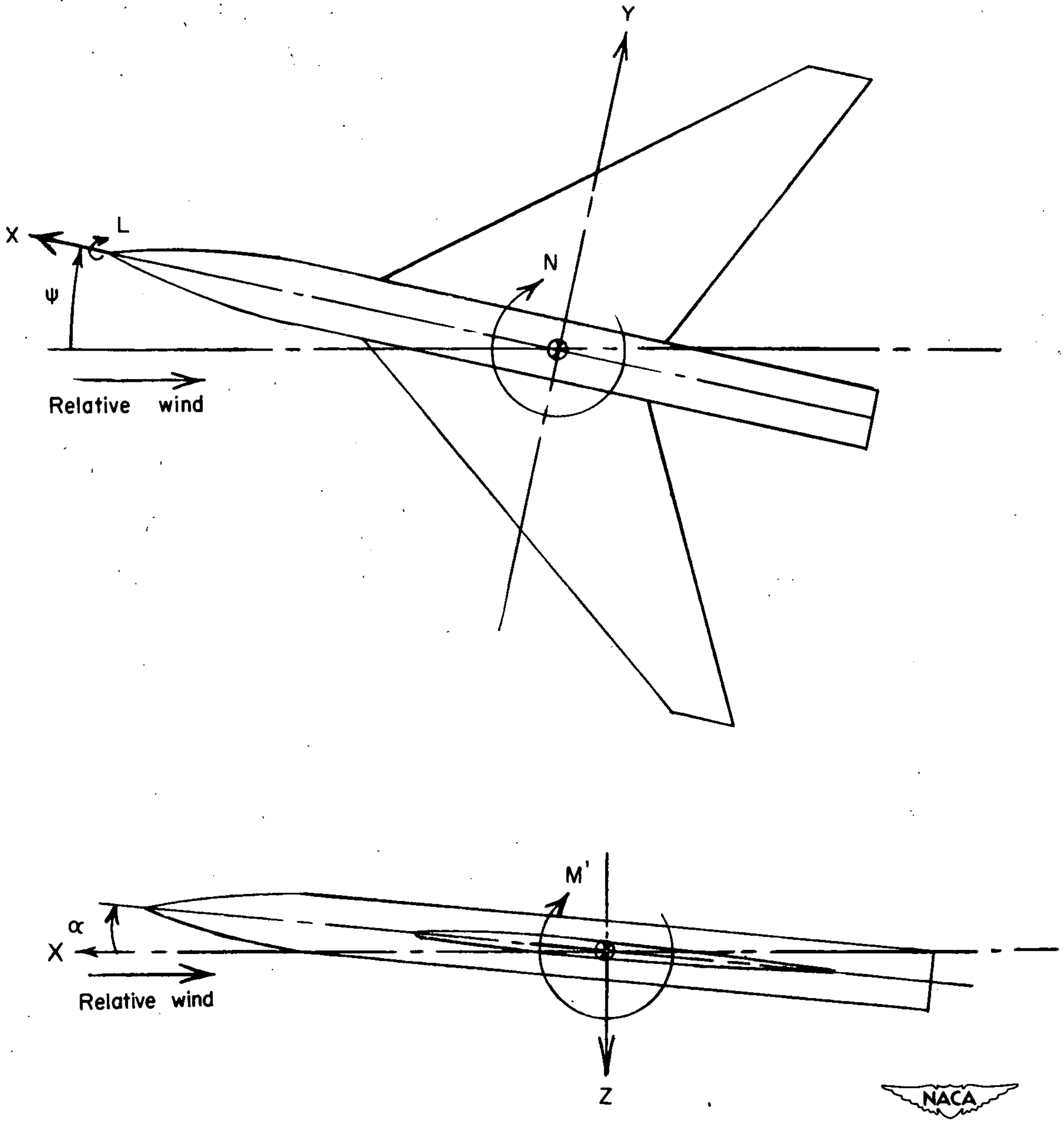

Figure 1.- System of stability axes. Arrows indicate positive values.

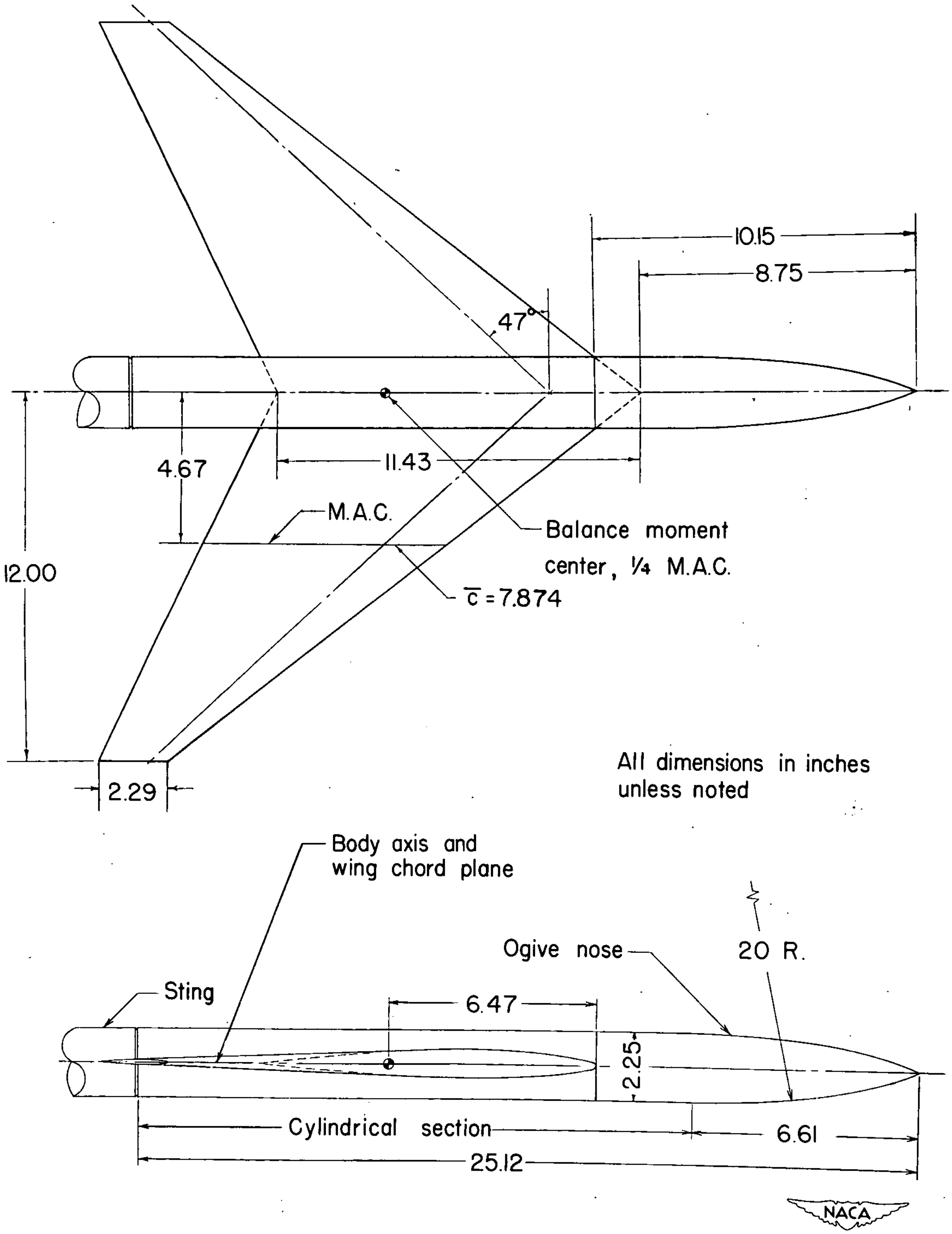

(a) Wing-body arrangement.

Figure 2.- Details of model configurations.

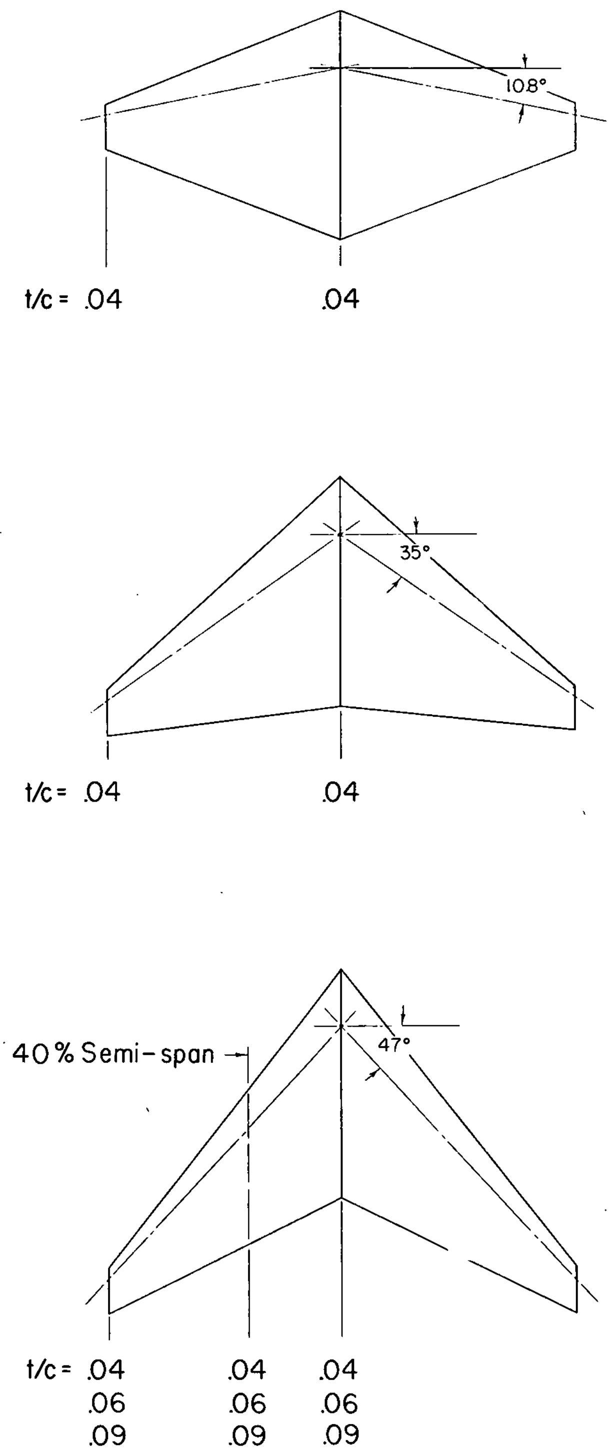

Aspect Ratio	3.5
Taper Ratio	0.2
Span, inches	24
Area, sq. feet	1.143

(b) Details of wings.

Figure 2.- Continued.

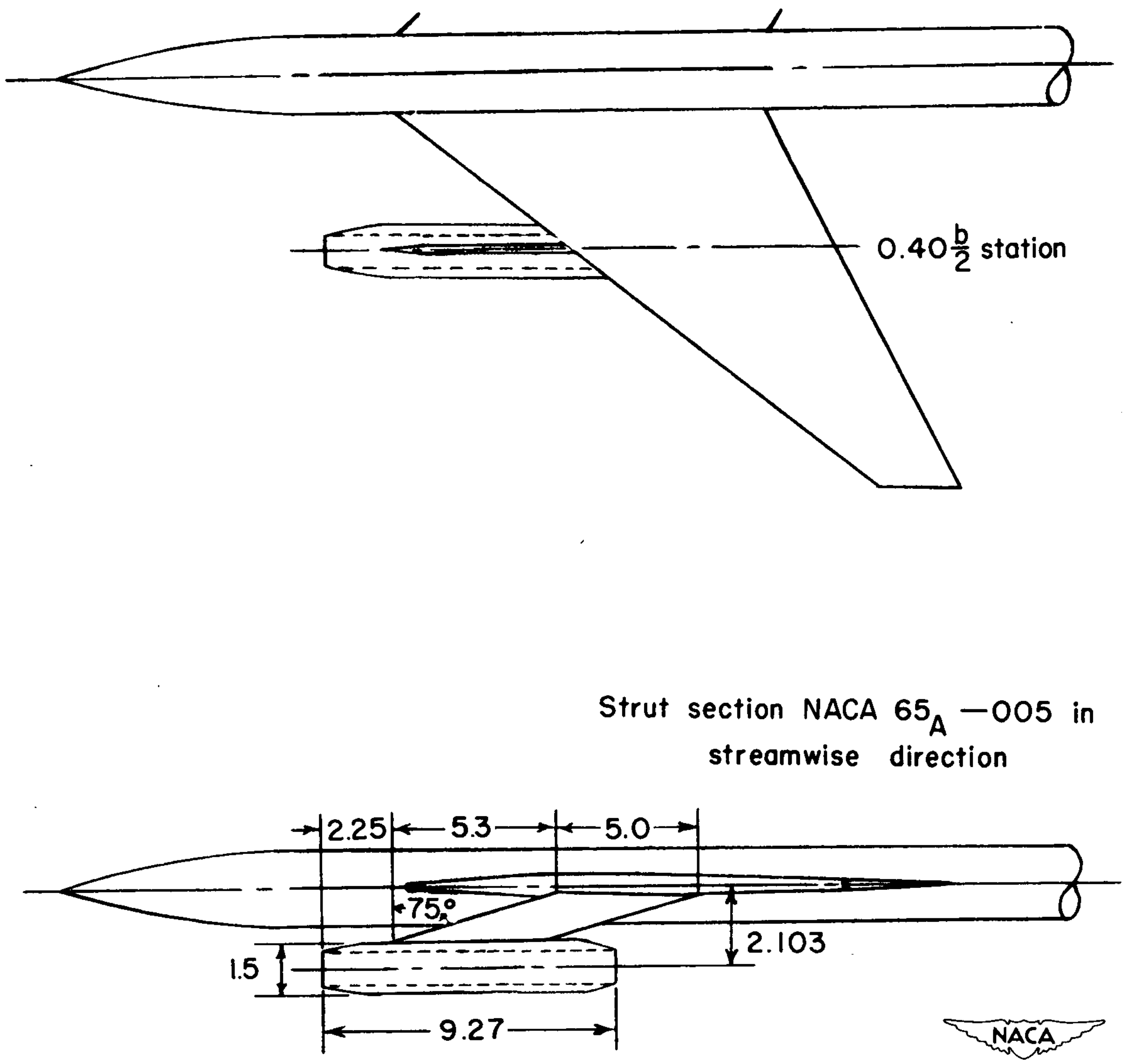

(c) Details of nacelle installation on $\Lambda = 47^{\circ}$; $\frac{t}{c} = 0.06$ wing.

Figure 2.- Concluded.

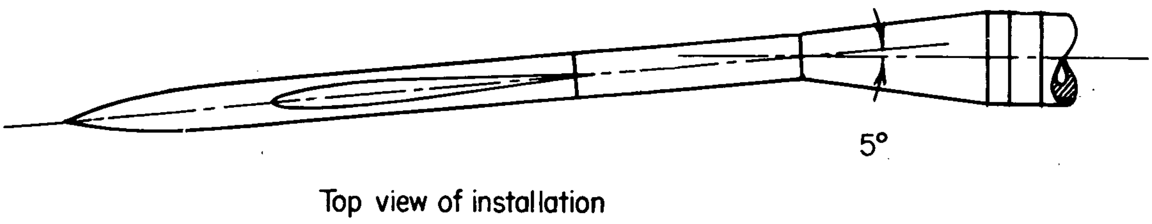

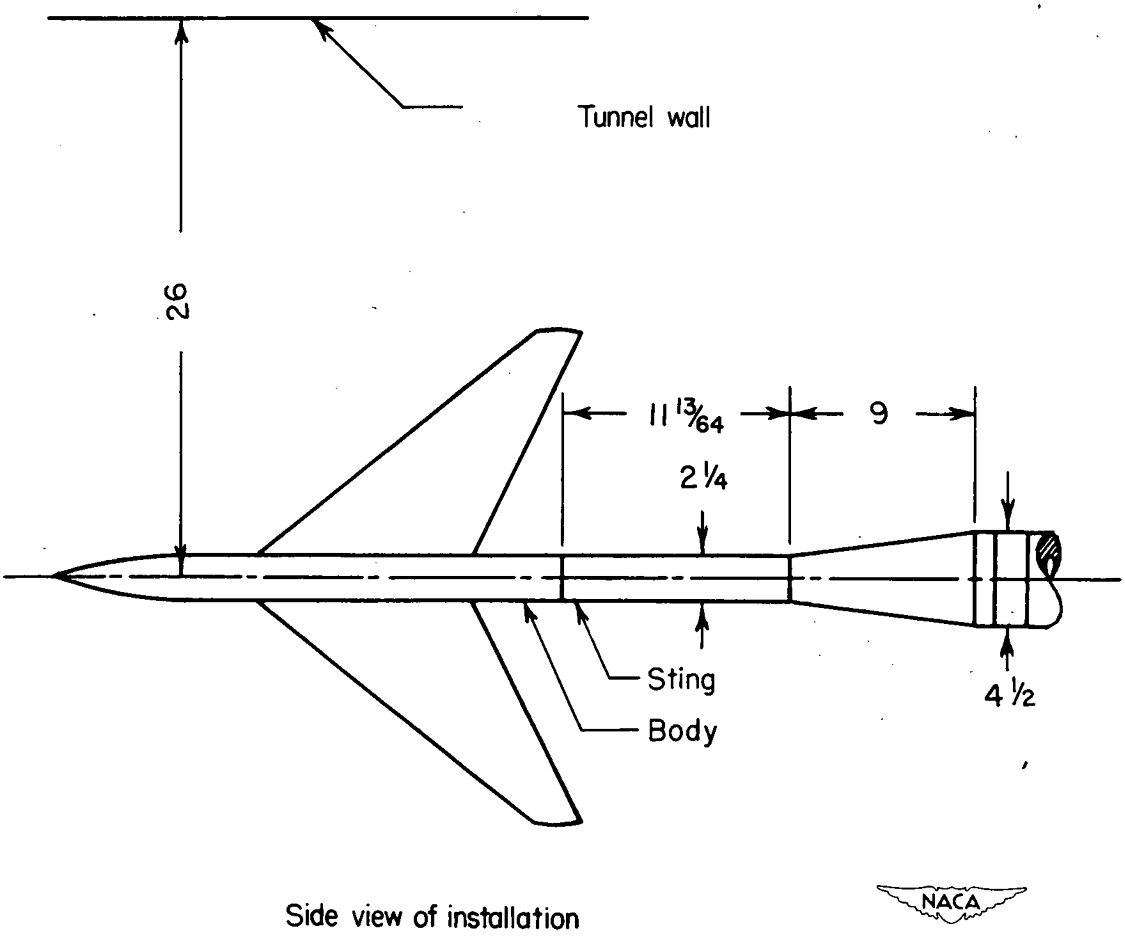

Figure 3.- Details of model sting support. All dimensions in inches unless noted.

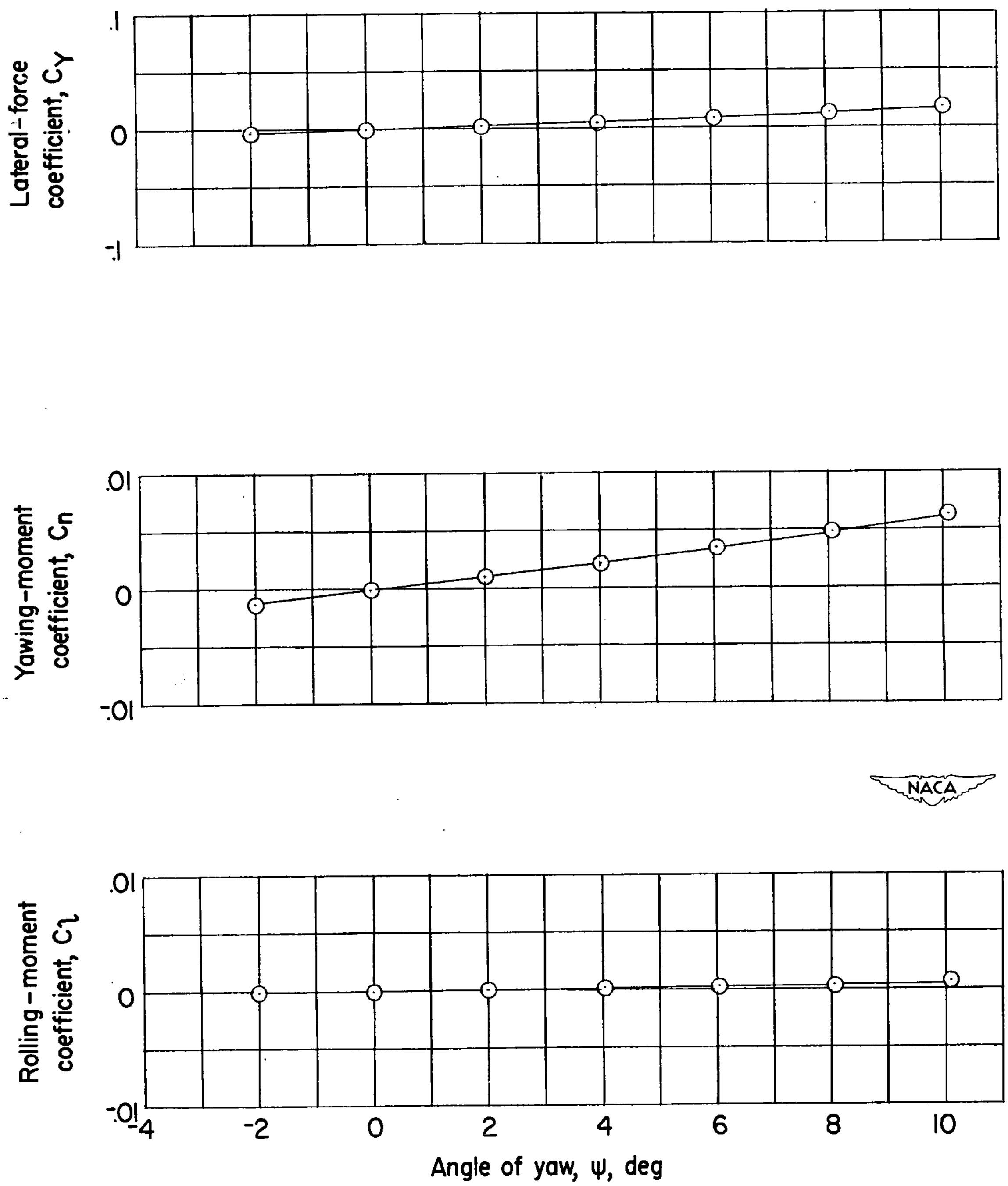

(a) Body alone.

Figure 4.- Aerodynamic characteristics in yaw for various configurations at $\alpha = 5^{\circ}$. $M = 1.60$.

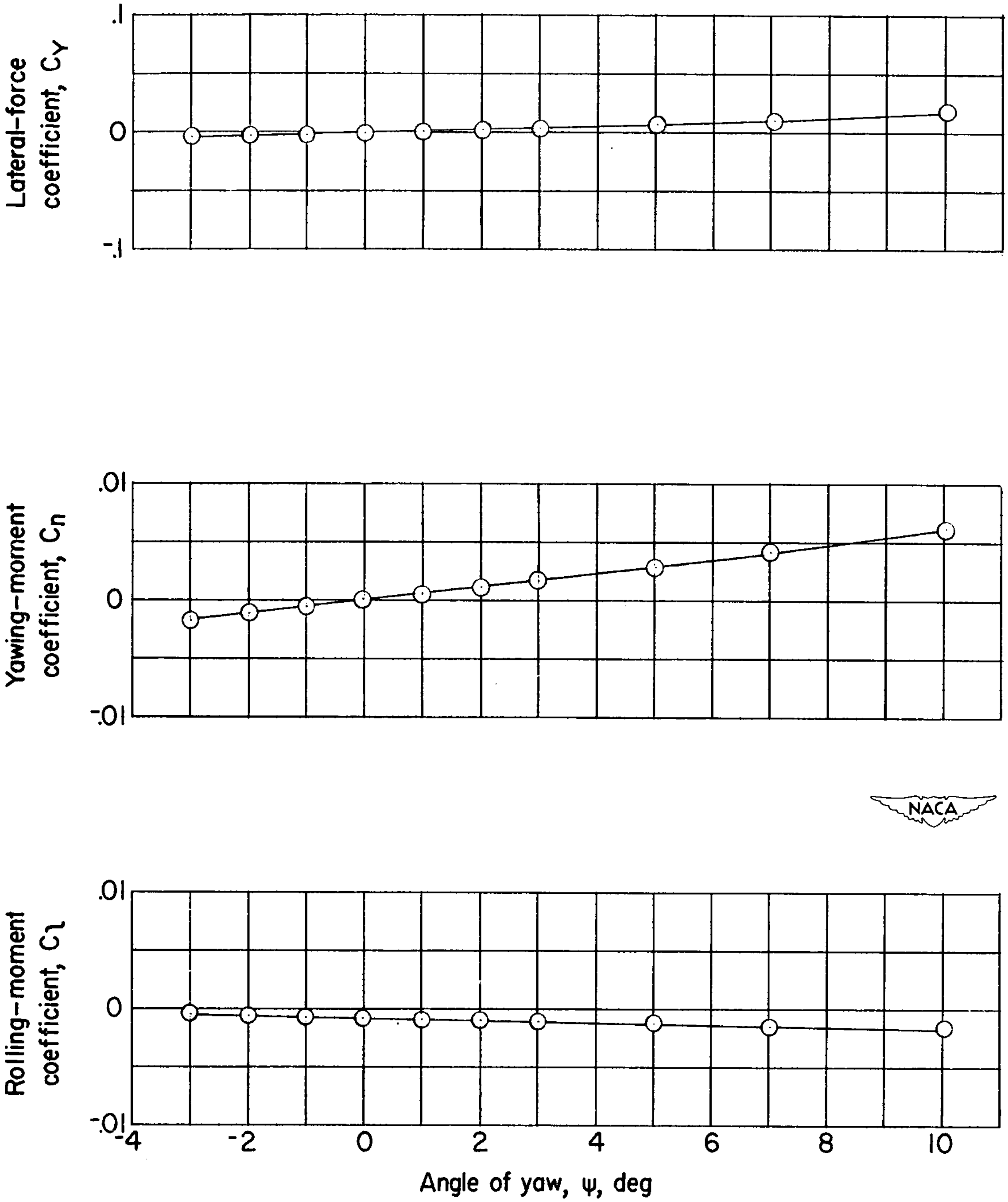

(b) $\Lambda = 10.8^{\circ}$; $\frac{t}{c} = 0.04$.

Figure 4.- Continued.

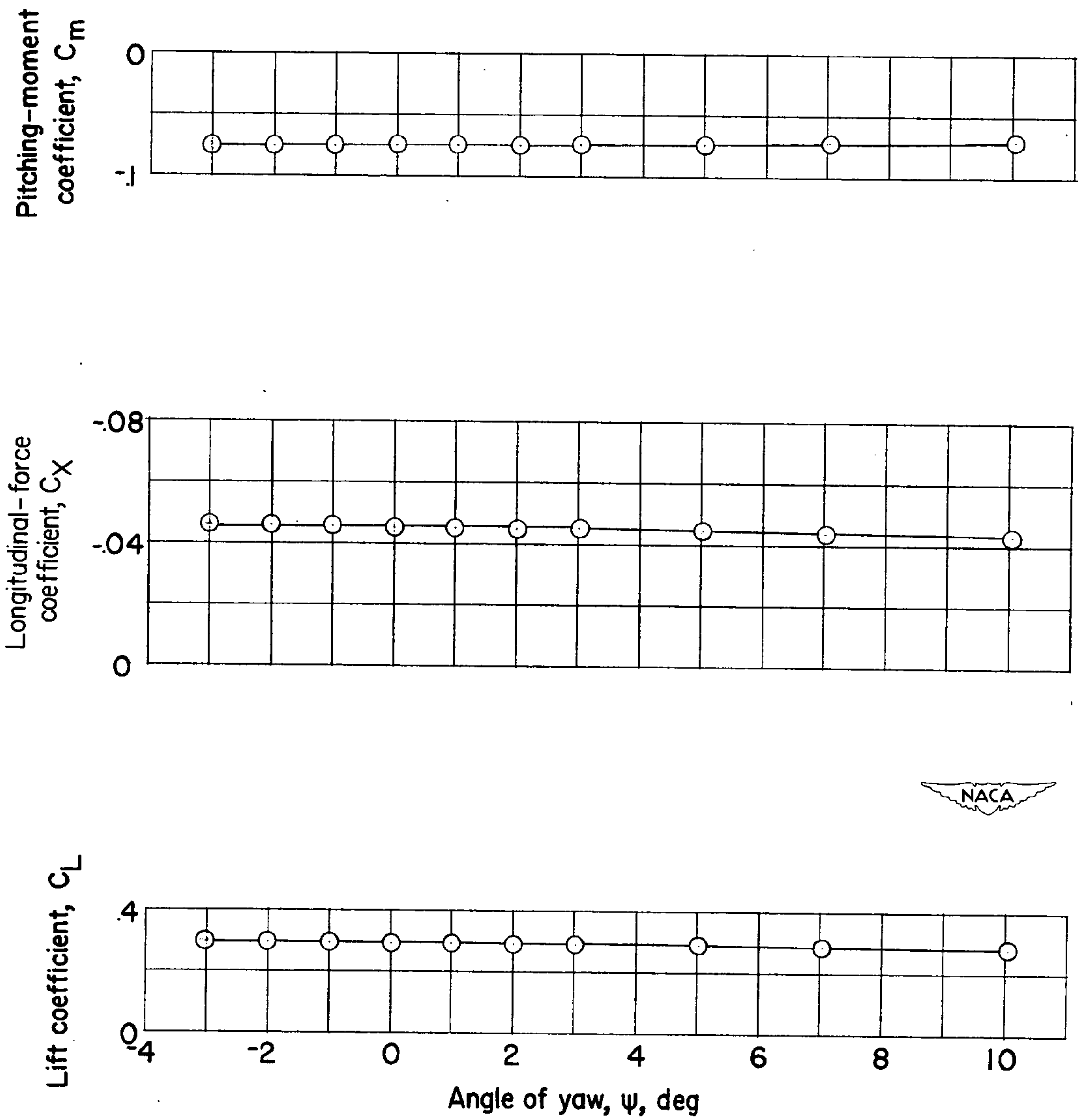

(b) Concluded.

Figure 4.- Continued.

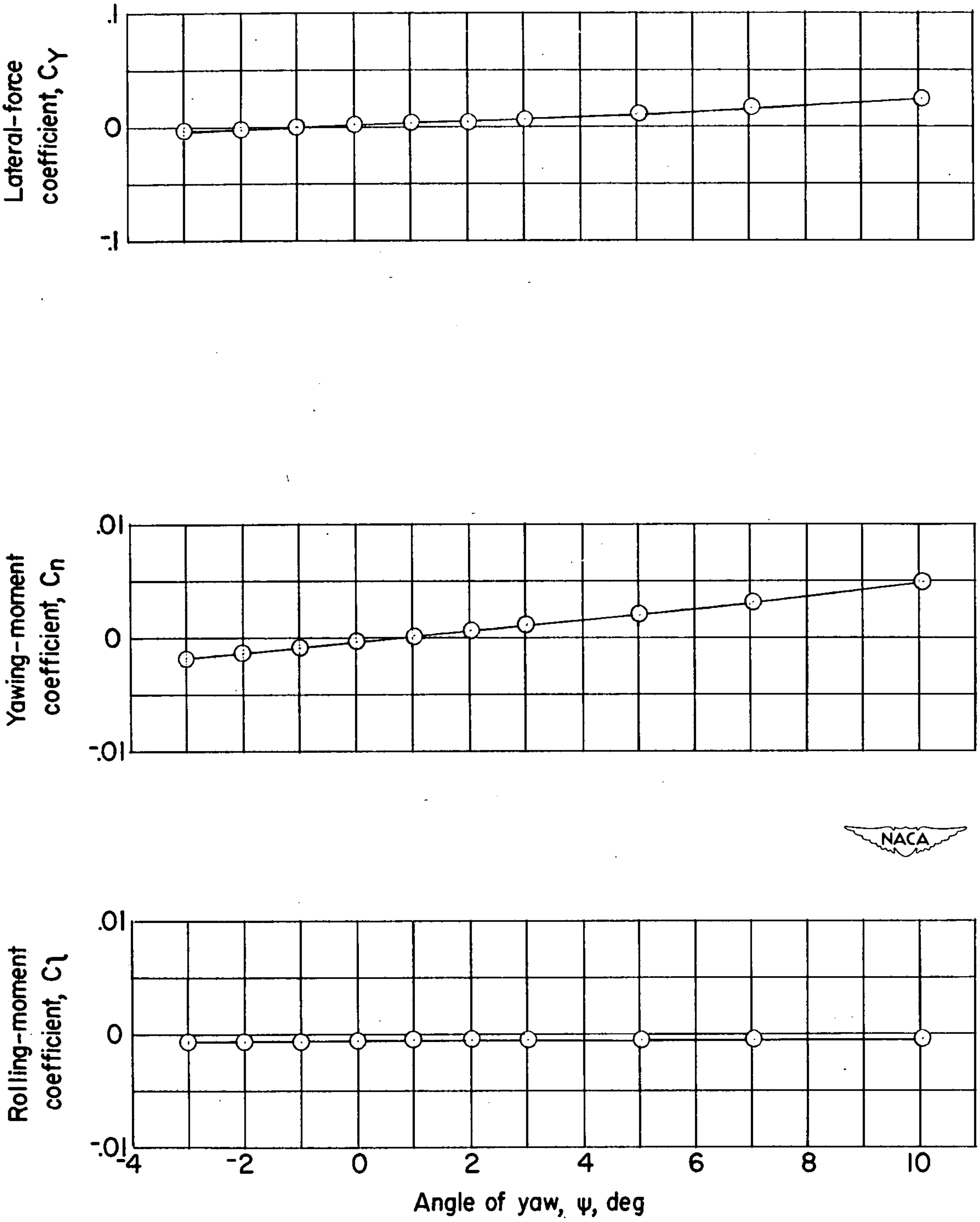

(c) $\Lambda = 35^{\circ}$; $\frac{t}{c} = 0.04$.

Figure 4.- Continued.

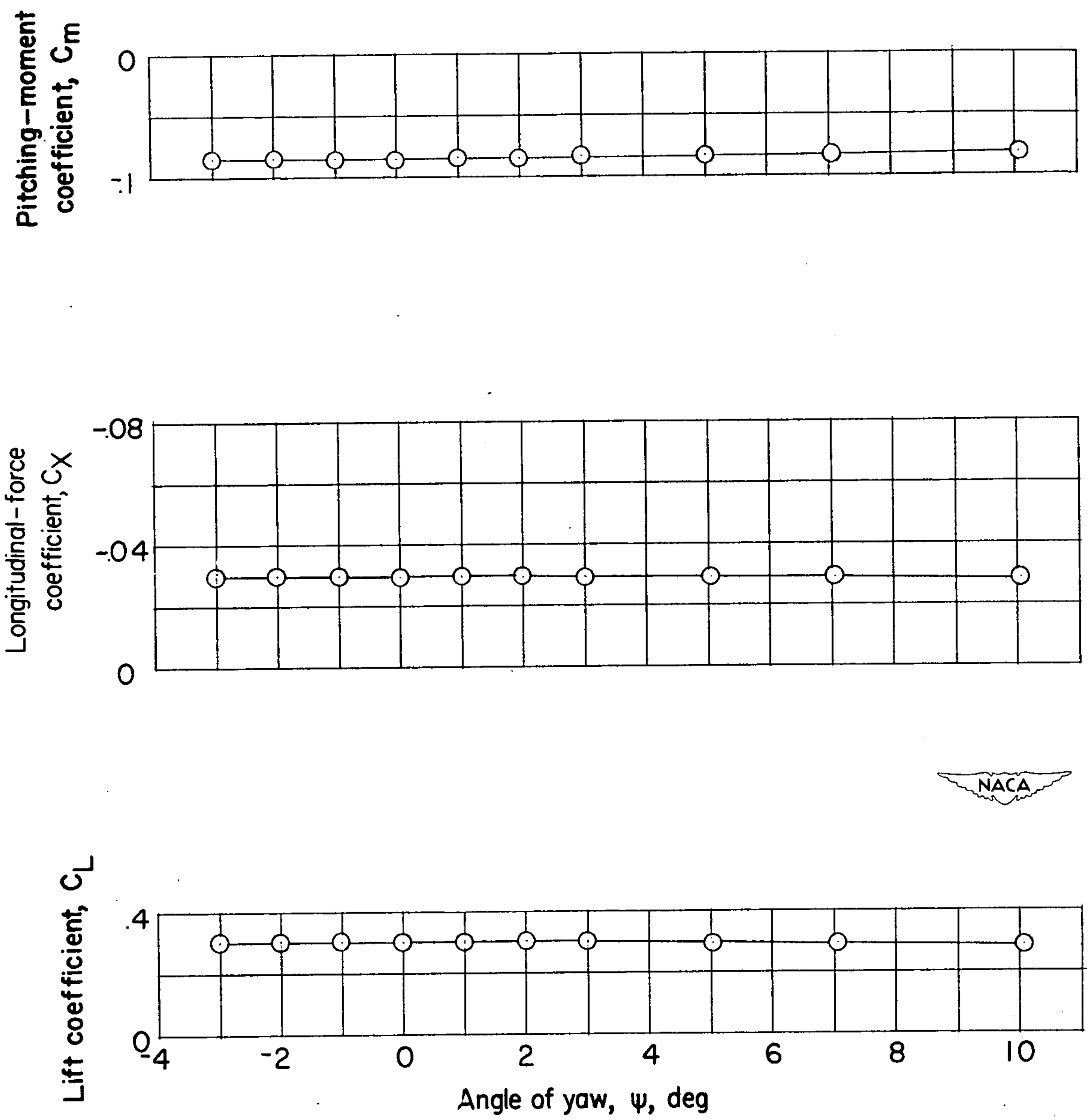

(c) Concluded.

Figure 4.- Continued.

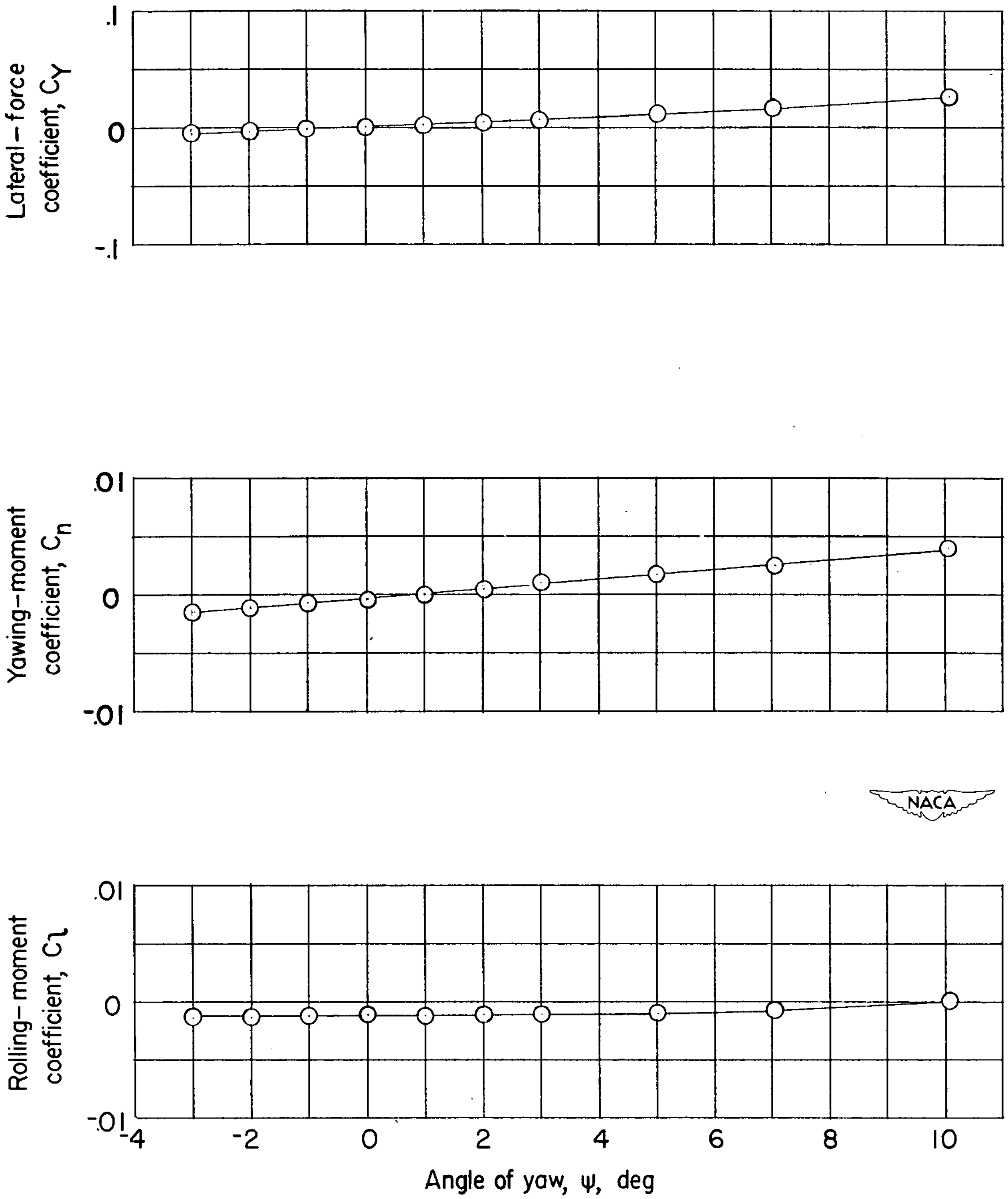

(d) $\Lambda = 47^{\circ}$; $\frac{t}{c} = 0.04$.

Figure 4.- Continued.

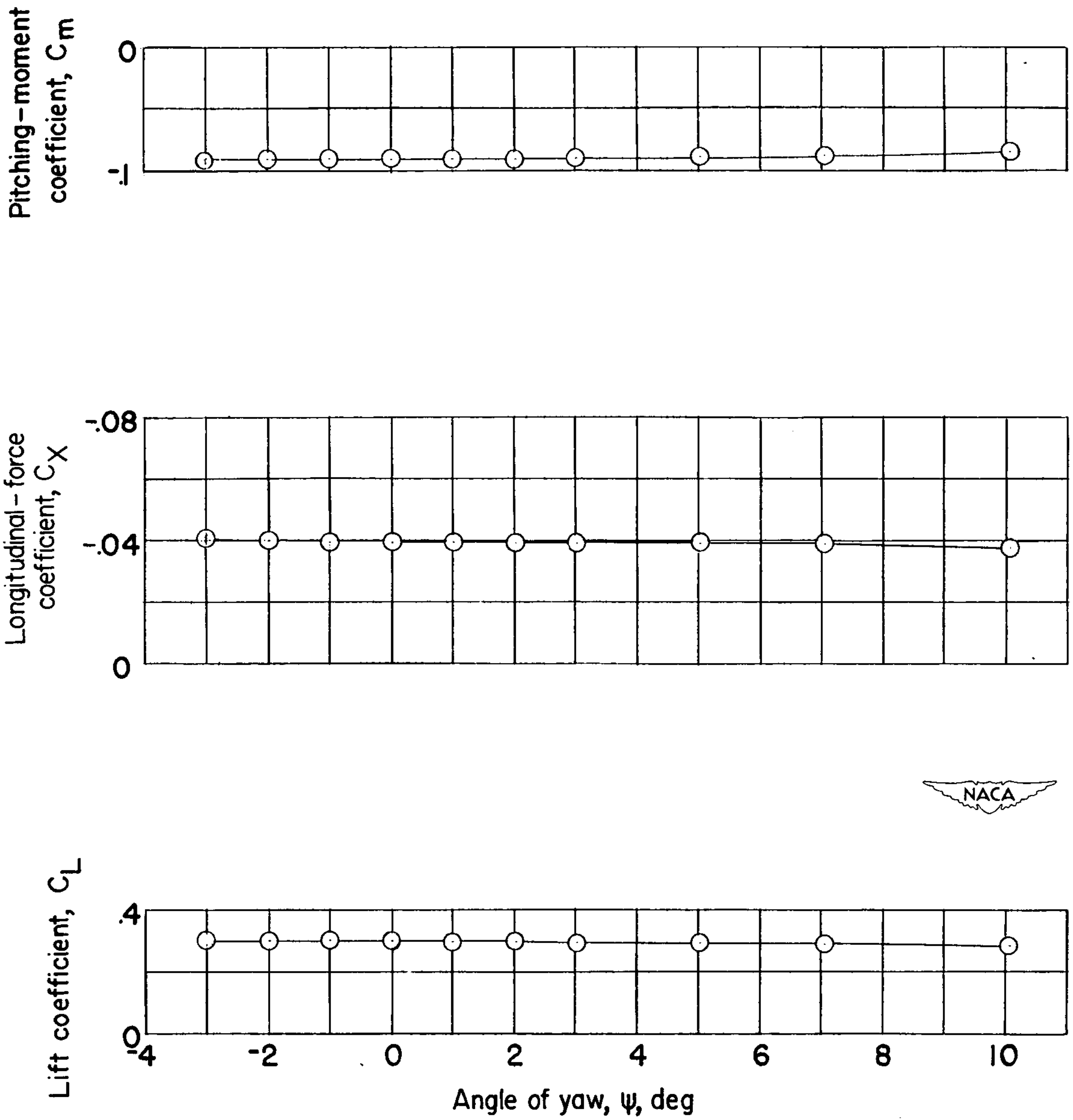

(d) Concluded.

Figure 4.- Continued.

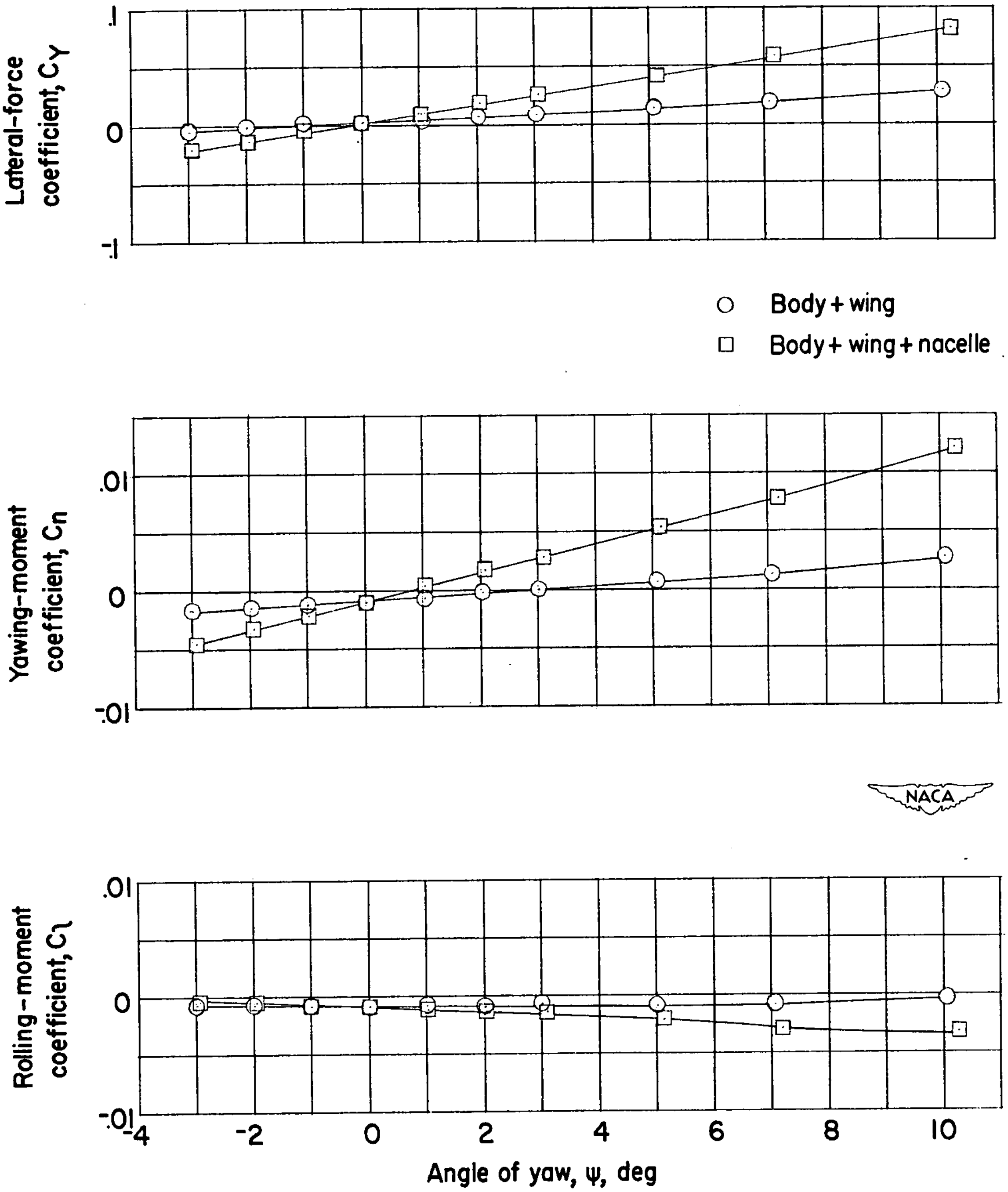

(e) $\Lambda = 47^{\circ}$; $\frac{t}{c} = 0.06$.

Figure 4.- Continued.

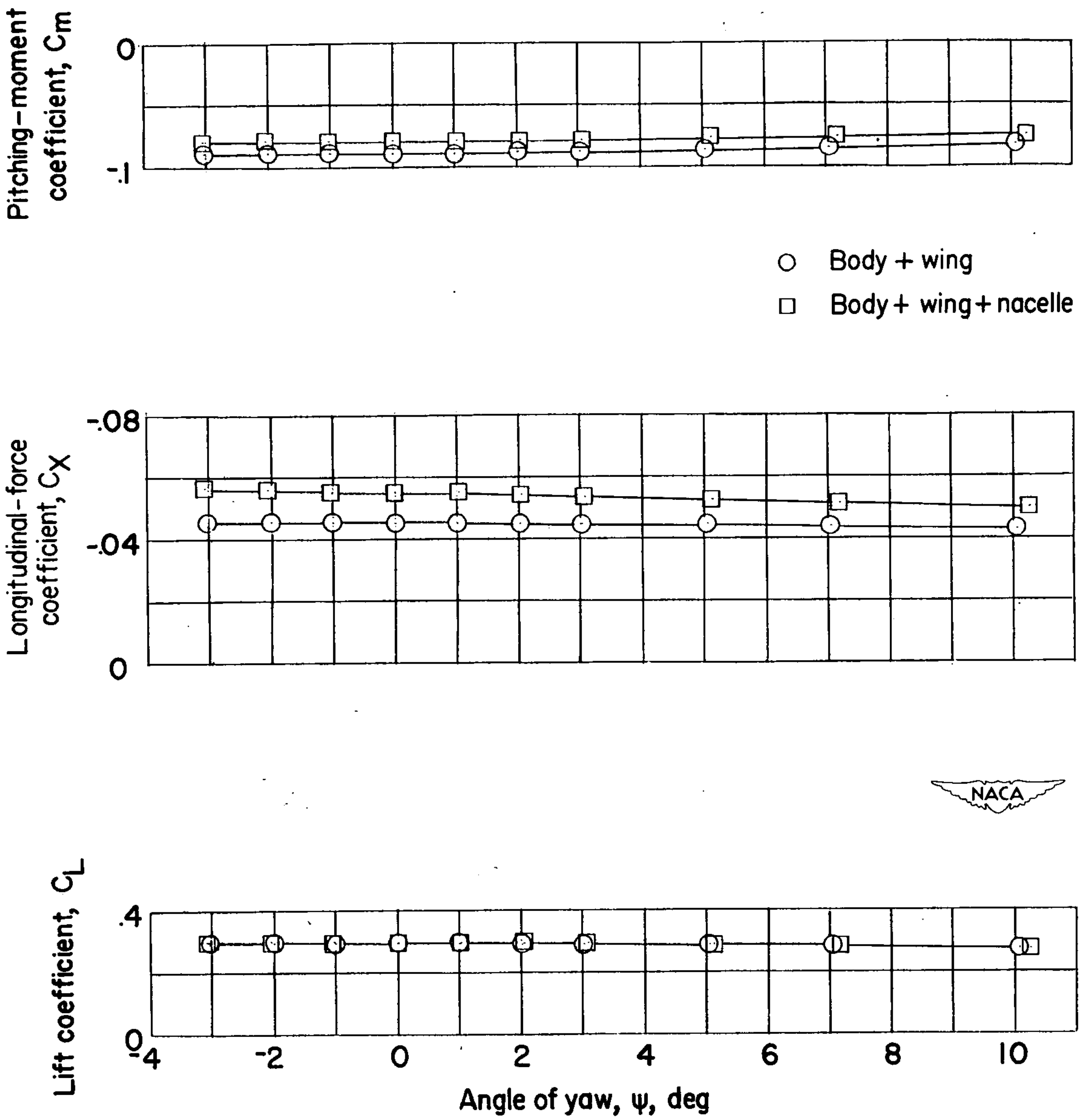

(e) Concluded.

Figure 4.- Continued.

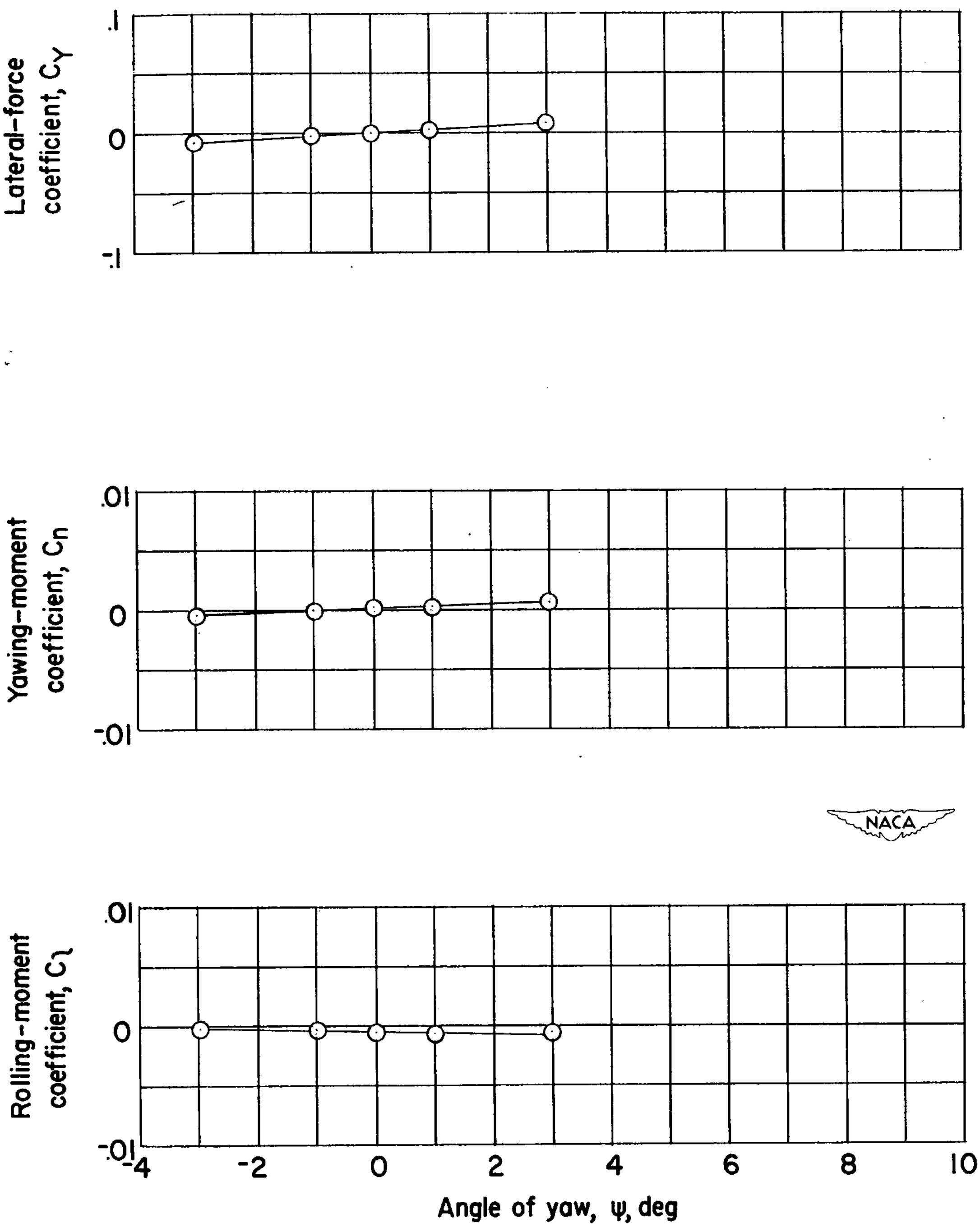

(f) $\Lambda = 47^\circ$; $\frac{t}{c} = 0.09$.

Figure 4.- Continued.

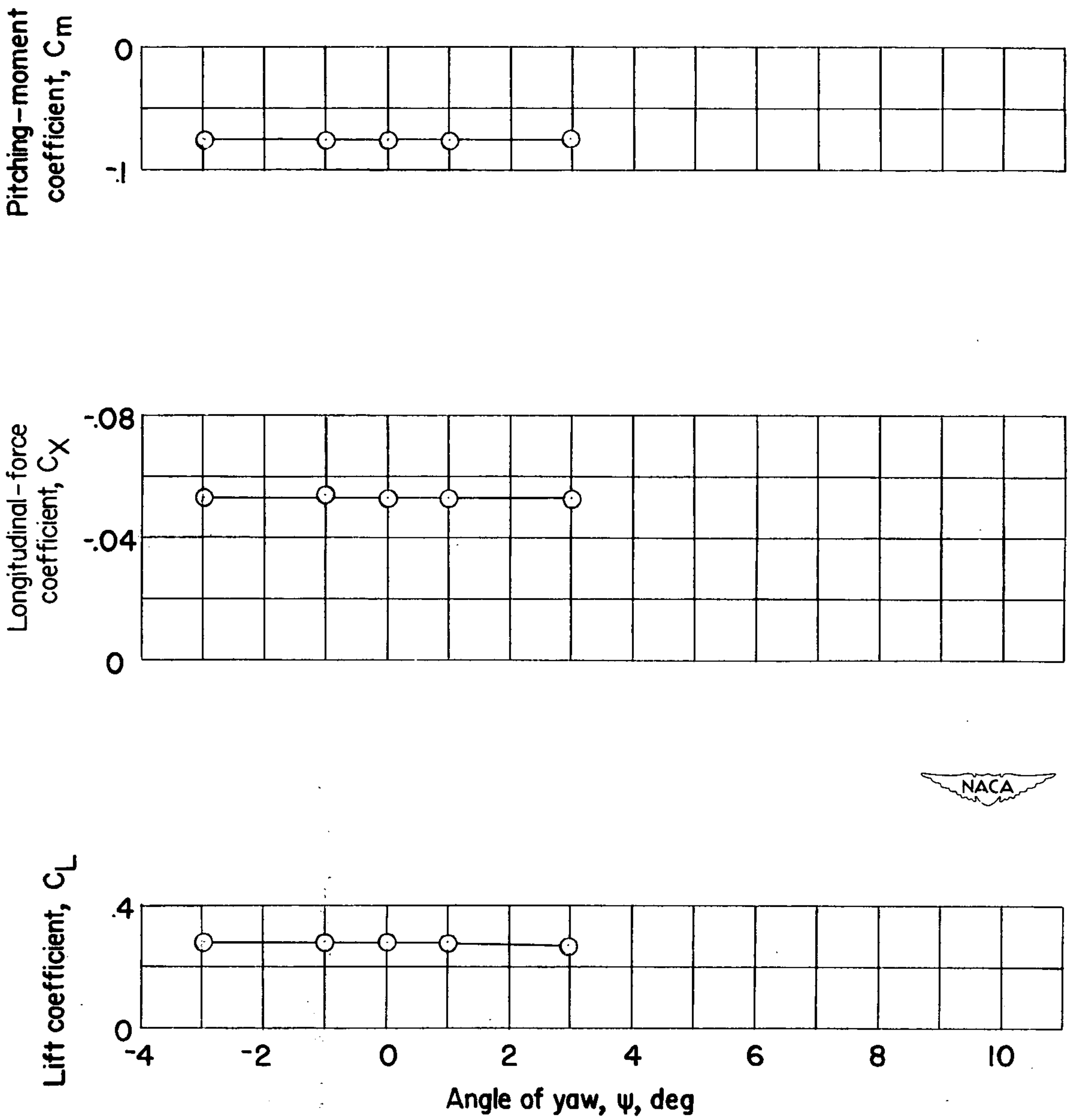

(f) Concluded.

Figure 4.- Concluded.

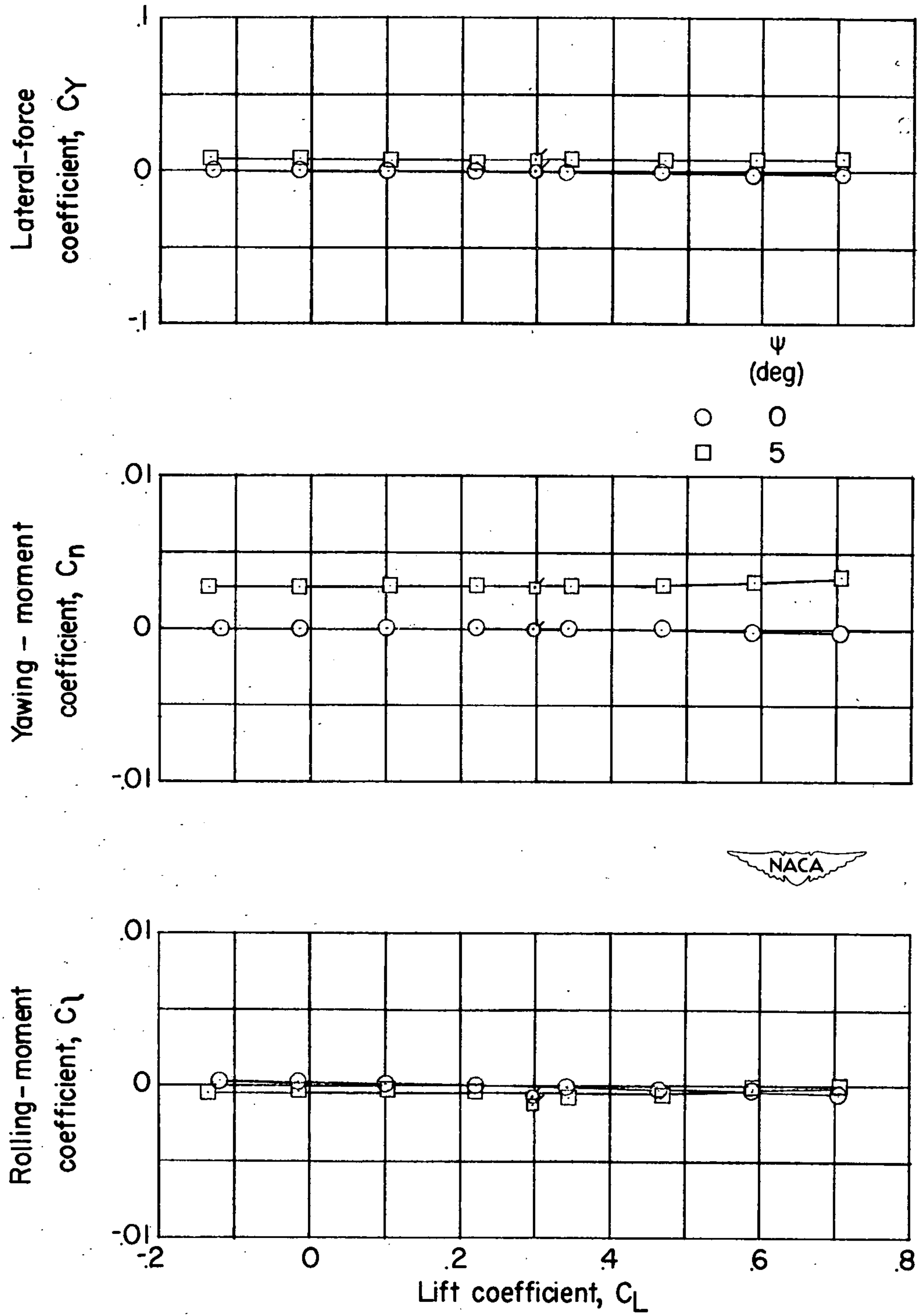

(a) $\Lambda = 10.8^{\circ}$; $\frac{t}{c} = 0.04$.

Figure 5.- Effect of yaw on the lateral characteristics in pitch for various configurations. Flagged symbols are values from yaw tests.

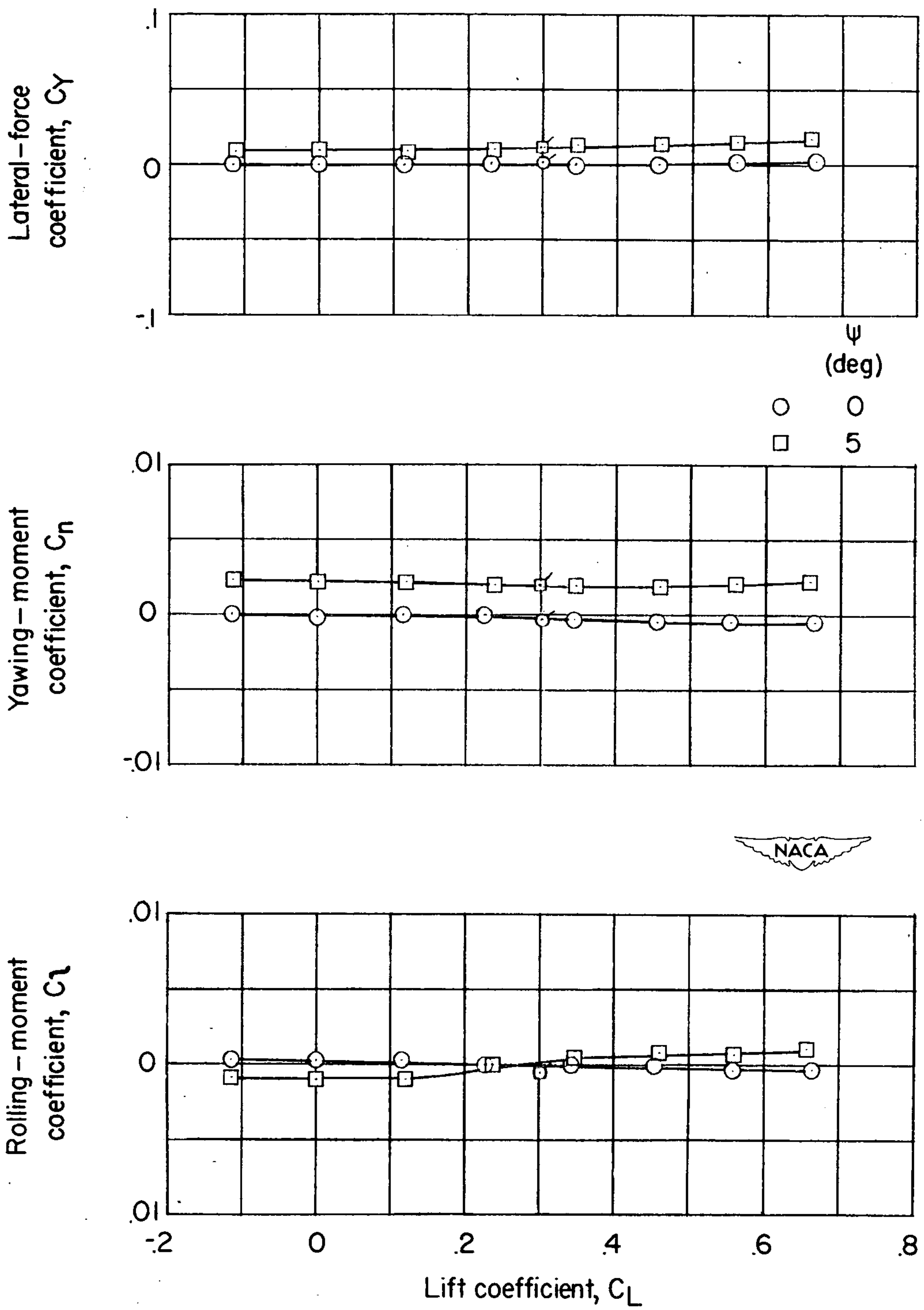

(b) $\Lambda = 35^{\circ}$; $\frac{t}{c} = 0.04$.

Figure 5.- Continued.

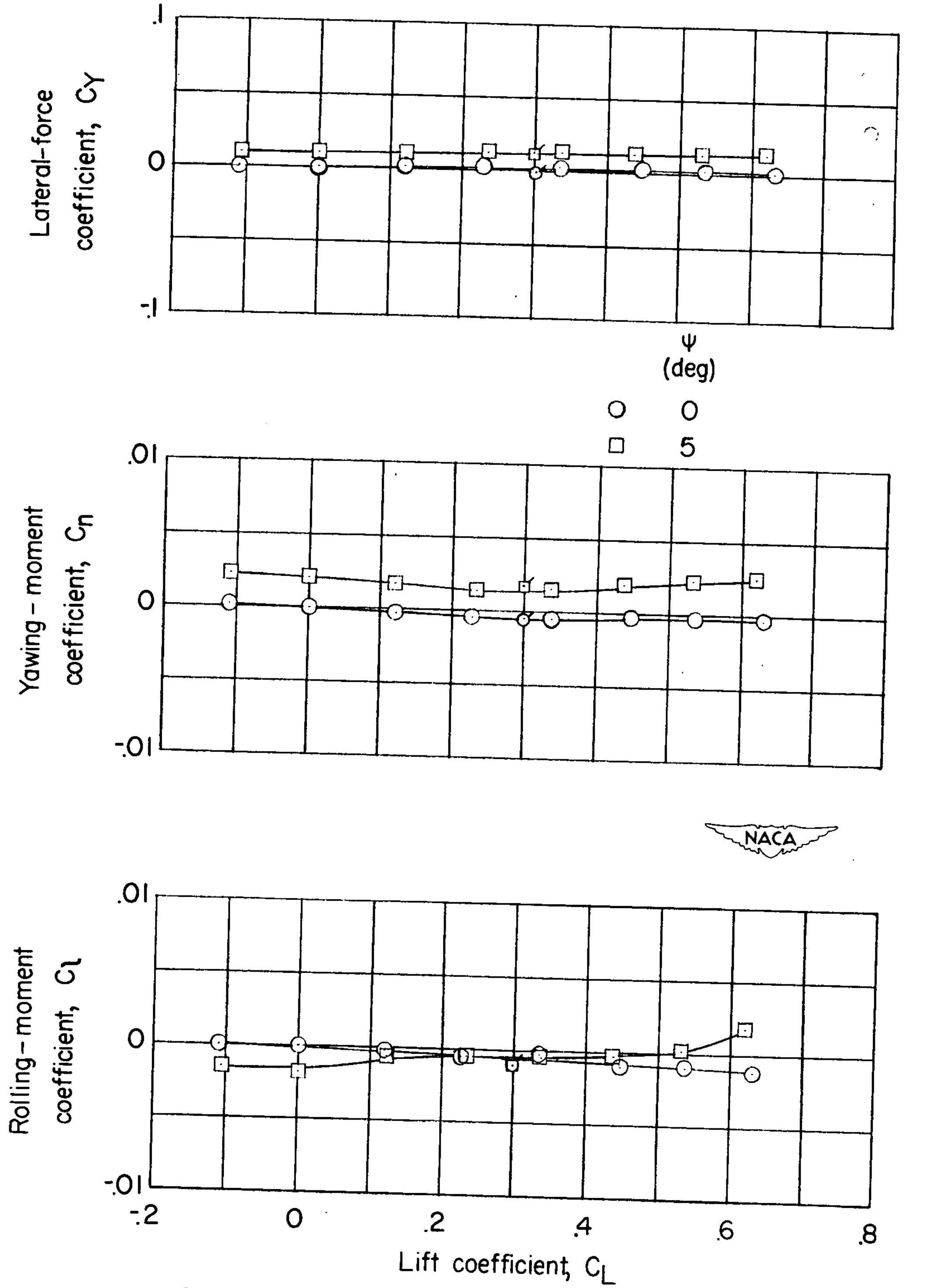

(c) $\Lambda = 47^{\circ}$; $\frac{t}{c} = 0.04$.

Figure 5.- Continued.

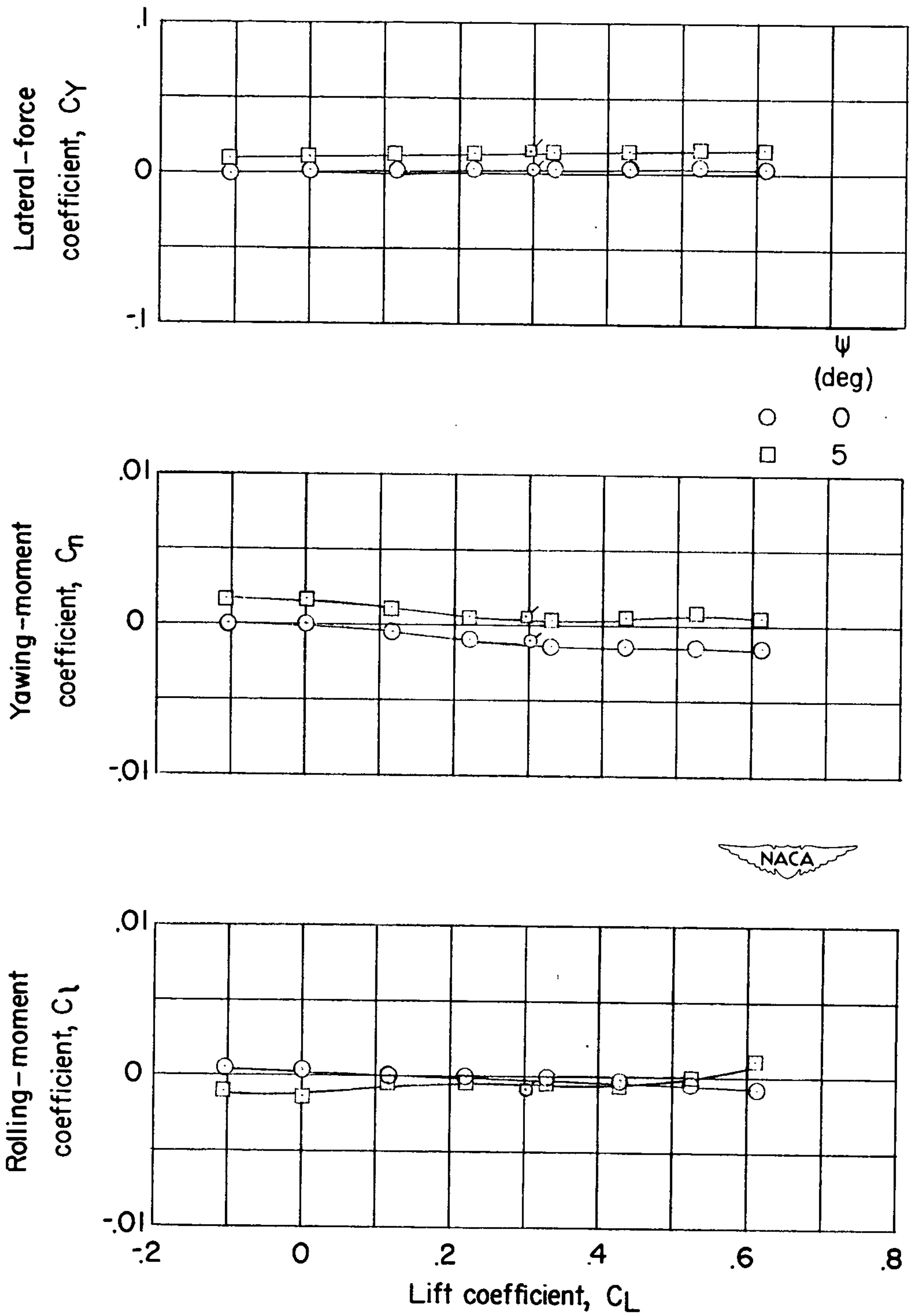

(d) $\Lambda = 47^{\circ}$; $\frac{t}{c} = 0.06$.

Figure 5.- Continued.

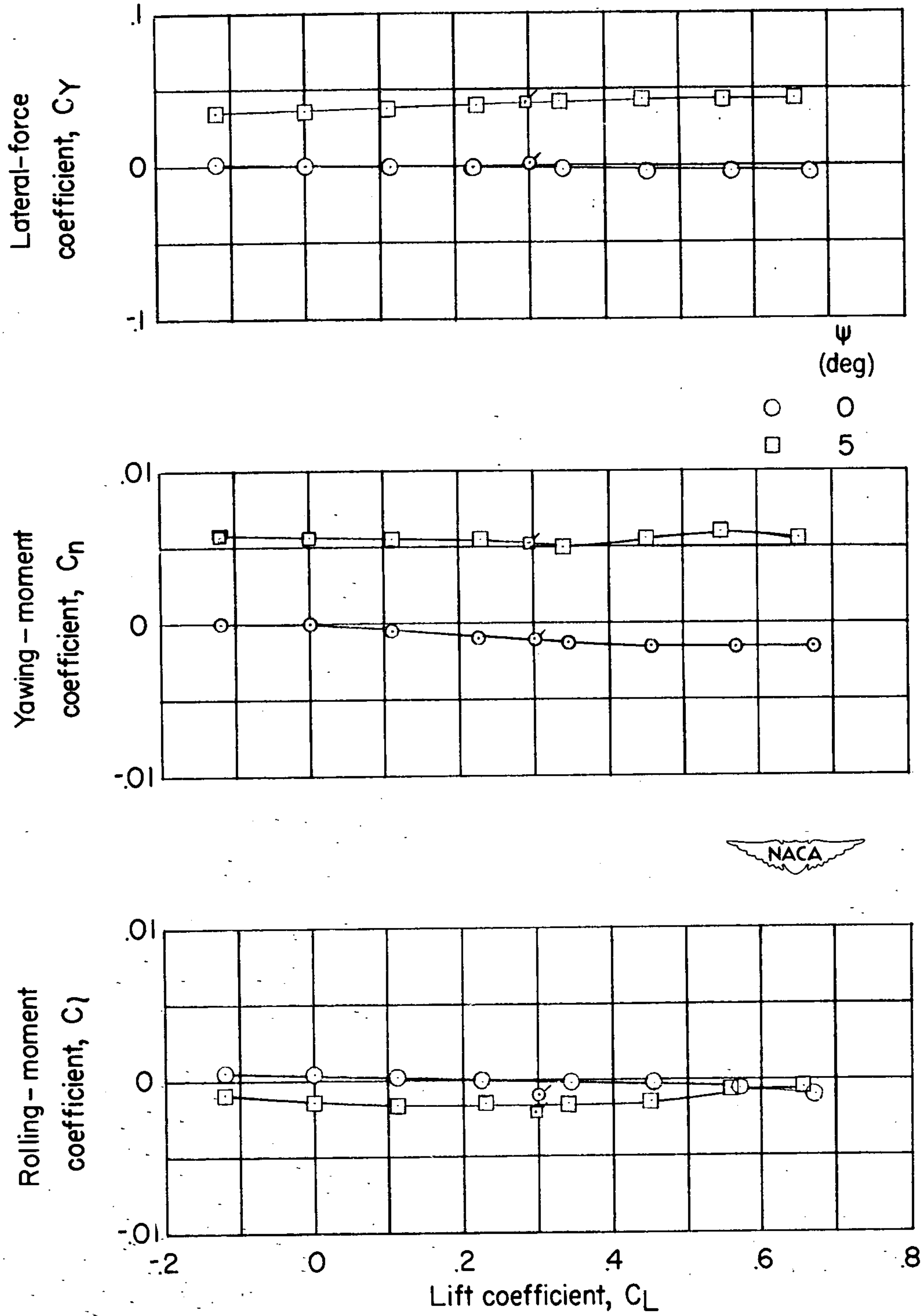

(e) $\Lambda = 47^{\circ}$; $\frac{t}{c} = 0.06$, nacelle on.

Figure 5.- Concluded.

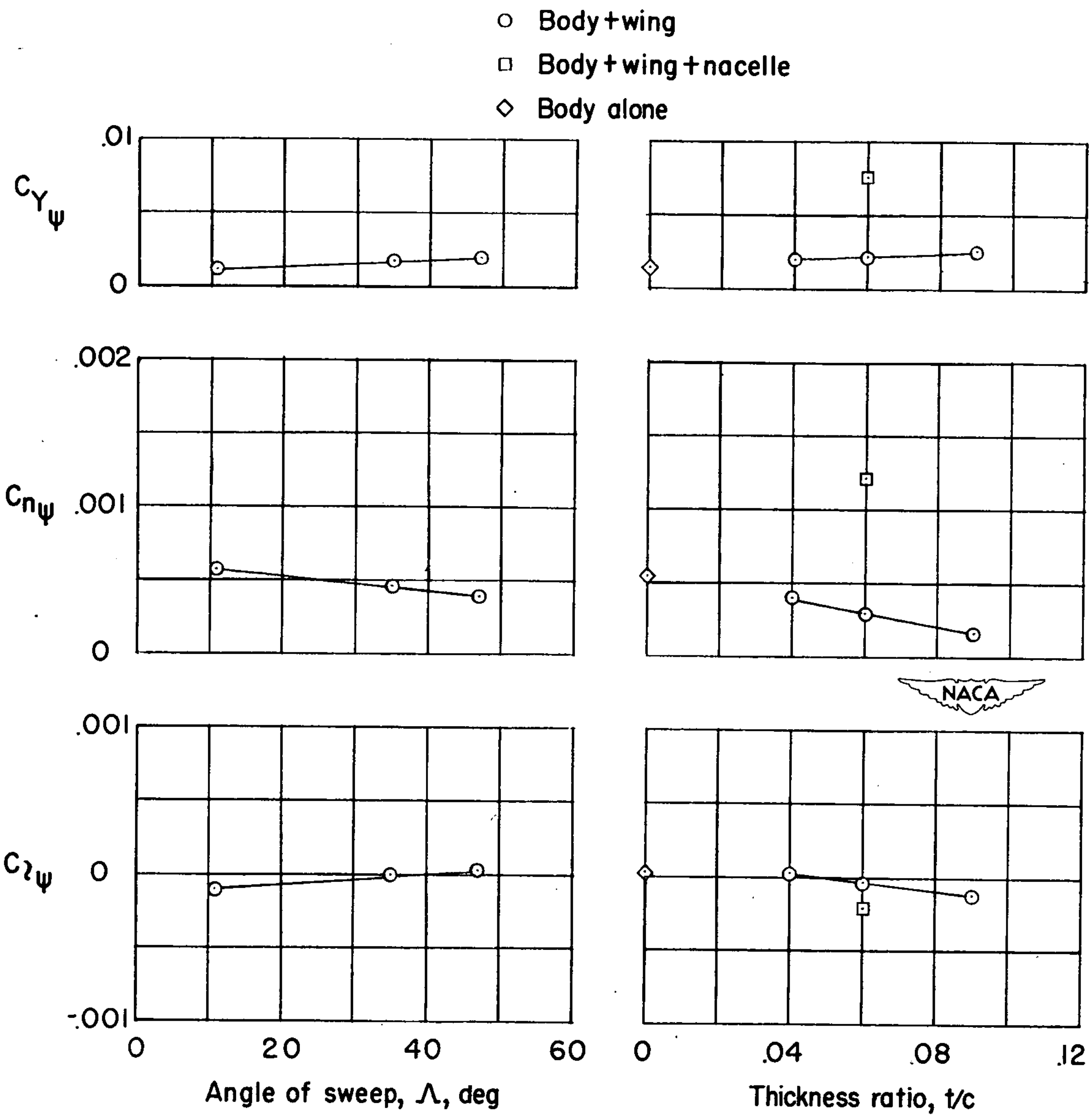

Figure 6.- Summary of the static lateral stability characteristics of various configurations at $\alpha = 5^{\circ}$. $M = 1.60$.